Indian Journal of Chemistry
Vol. 59A, March 2020, pp. 317-323

Synthesis and characterization of 2-aminoethylphosphonic acid-functionalized graphene quantum dots: biological activity, antioxidant activity and cell viability

Gönül Yapar[a,*], Behiye Şenel[b], Neslihan Demir[c] & Mustafa Yıldız[d,*]

[a]Department of Chemistry, Faculty of Arts and Sciences, Istanbul Technical University, Istanbul 34469, Turkey

[b]Department of Pharmaceutical Biotechnology, Faculty of Pharmacy, Anadolu University, Tepebaşı-Eskişehir, TR 26470, Turkey

[c]Department of Biology, Faculty of Arts and Sciences, Çanakkale Onsekiz Mart University, Çanakkale 17100, Turkey

[d]Department of Chemistry, Faculty of Arts and Sciences, Çanakkale Onsekiz Mart University, Çanakkale 17100, Turkey

Email: yaparg@itu.edu.tr (G Y)/ myildiz@comu.edu.tr (M Y)

Received 18 February 2019; revised and accepted 10 February 2020

A facile, environmentally friendly one-step reaction for the preparation of luminescent N-doped graphene quantum dots (GQDs) involving a hydrothermal reaction between citric acid and 2-aminoethylphosphonic acid has been designed. Graphene quantum dots have been characterized by UV-visible absorption, FTIR spectroscopy, transmission electron microscopy (TEM), energy dispersive X-ray spectroscopy (EDX) and dynamic light scattering (DLS) techniques. Furthermore, the biological activity of the GQDs has been studied. UV-visible spectroscopy studies of the interactions between the GQDs and calf thymus DNA (CT-DNA) showed that the compound interacts with CT-DNA via intercalative binding. DNA cleavage study showed that the GQDs cleaved DNA oxidatively. In addition, antioxidant activity of N-doped GQDs was measured using the DPPH method. As the concentration of the compound increased, the antioxidant activity also has increased. According to cell viability analyses results, the N-doped GQDs showed cell viability (70%) when the concentration reaches 228 μg/mL for A549, 200 μg/mL for MDA-MB-231 and 140 μg/mL for NIH-3T3 cell lines with 24 h incubation.

Keywords: N-doped graphene quantum dots, Biological activity, Antioxidant activity, MTT, Cell viability

Graphene quantum dots (GQDs), which are a very interesting type of zero-dimensional luminescent nanomaterial, are small graphenes with a quantum size between 2 and 20 nm[1]. In the last few decades, quantum dots have gained a special status among nanomaterials and made significant progress with ever-increasing research, but in recent years, graphene-based nanomaterials have become a topic of more scientific interest[2,3]. The p–p bonds below and above the atomic plane give graphene exceptional thermal and electrical conductivity[2].

For the last decade, GQDs have been widely studied due to their excellent photoluminescent properties, high water solubility, optoelectronic properties, minimal toxicity, corrosion resistance, and in vitro and in vivo biocompatibility. GQDs exhibit good biocompatibility, excellent chemical inertness and non-toxicity, like graphene[4-6]. The biocompatibility of graphene quantum dots was investigated for the applications in photodynamic therapy[7]. High reactive oxygen species are required for photodynamic therapy, and it is very difficult to produce high reactive oxygen species for the same. The results of the study support the potential of GQDs for future photodynamic therapy applications, providing enhanced reactive oxygen species production combined with good biocompatibility and minimal toxicity in vitro and in vivo[7]. These properties along with suitable photoluminescent properties make GQDs promising materials for treatment of some specific illnesses. The optical properties of GQDs are largely dependent on particle sizes, so the energy band spacing of the GQDs can be adjusted by modulating their size[8].

Biomedical applications of nanomaterial based on GQDs were implemented in many areas, particularly for diagnostics[9,10], drug delivery[11], in vitro and in vivo bio-imaging[12-15]. These studies have shown that GQDs are promising candidates for the future applications. At the same time, graphene quantum

dots were studied as a probe for programmatically monitoring anticancer drug delivery, release and response[2]. In the study, the researchers have developed a new type of invasive agent by loading the anticancer drug doxorubicin (DOX) onto the surface of the GQD and loading Cy5.5 dye with a cathepsin D-responsive peptide into the GQD[16].

The development of new antioxidants with rapid absorbency of free radicals and excellent biocompatibility are among the most studied topics in recent years. GQDs are one of the most promising candidate antioxidants because of their unique structure, excellent biocompatibility and low toxicity. Therefore, antioxidant mechanisms were investigated by focusing on the relationship between antioxidant activity and surface oxygen functional groups on GQDs[17]. The rapid increase in studies about GQDs has shown that these nanomaterials may have antioxidant[18-21], antimicrobial[21-23] and cytotoxic effects[21,24,25], not just biosensing. For example, the effects of chemical compositions of some GQDs on antioxidant and free radical scavenging activities were investigated and compared[20,21,26]. The inhibitory effective concentration of the best performing GQDs was found to be lower than ascorbic acid and other carbon nanomaterials[20]. Thus, there are very few antioxidant studies about N-doped GQDs and GQDs. Like antioxidants, there are very few DNA binding and DNA cleavage studies about N-doped GQDs and GQDs. GQDs may also be useful as chemotherapeutics for cancer treatment and for stem cell differentiation and imaging[27]. In addition, some GQDs have been found to have biocompatible properties against A549 or HeLa cells up to 200 µg/mL[28,29]. In this study, graphene quantum dots (GQDs) containing N atoms were synthesized[30,31] using the hydrothermal reaction of citric acid and 2-aminoethylphosphinic acid (Scheme 1). The compound was characterized with TEM, DLS, EDX, UV-visible and FTIR spectroscopy. The interaction with DNA was investigated by UV-visible spectroscopy and the agarose gel electrophoresis method. Antioxidant properties were also investigated using DPPH (2,2-diphenyl-1-picrylhydrazyl hydrate) free radical assay. Moreover, the cell viability of N-doped GQDs were examined for various cell lines.

Materials and Methods

Materials

All chemicals were obtained from commercial sources and used without further purification. Citric acid (CA), 2-aminoethylphosphinic acid (2-AEPA), 2,2-Diphenyl-1-picrylhydrazyl (DPPH), butylated hydroxytoluene (BHT), silica gel 60 (0.063-0.200 mm), ethidium bromide (EB), calf thymus DNA (CT-DNA) and pBR322 DNA were purchased from Sigma-Aldrich.

Infrared absorption spectra were obtained from a Perkin Elmer BX II spectrometer in KBr pellets. UV-visible spectra were measured using PG Instruments T+80 UV/vis spectrophotometer. Morphology and crystal structure of nanoparticles were characterized using Transmission Electron Microscopy (TEM: JEM1010-JEOL). Chemical composition of samples was determined by JEOL Scanning Electron Microscope/Energy Dispersive X-ray JEOL TEM-1400-EDX instrument. The dynamic light scattering for particle size determination were carried out at 90° angle detector using DLS (Brookhaven Ins. and Cor. 90 plus) particle size analyzer, with 35 mW solid state laser detector operating at a wavelength of 658 nm.

Synthesis of N-doped GQDs

Citric acid (1.20 g, 6.25 mmol) and 2-aminoethylphosphinic acid (0.80 g, 6.40 mmol) were dissolved into 50 mL distilled (DI) water. The solution was transferred to an autoclave and heated at 250 °C for 4 h. Then, the mixture was evaporated and the crude

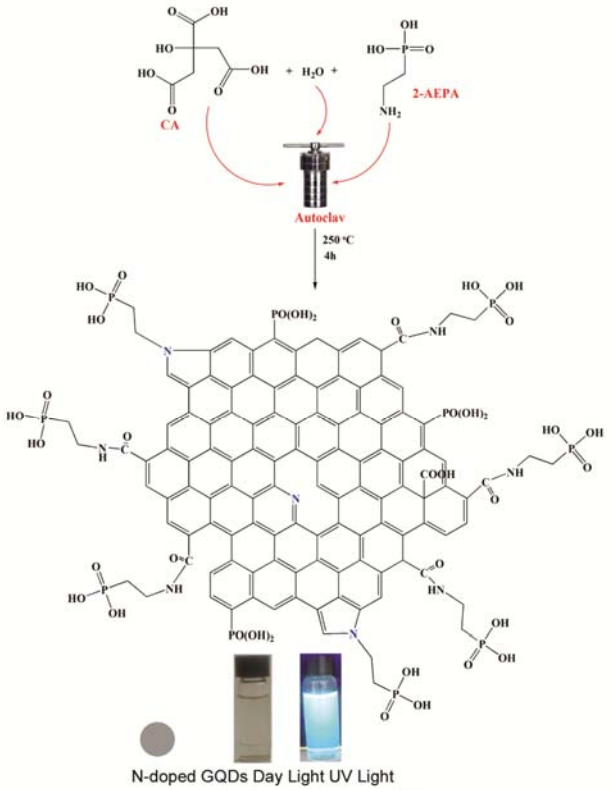

Synthesis of N-doped GQDs.

Scheme 1

product was subjected to column chromatography (silica gel 60 g, eluent; $CHCl_3$:Ethanol, 3:1) for separating the compound. The supernatant containing graphene quantum dots (GQDs) were collected. Compound was obtained from the evaporation of solution.

DNA-Binding experiments

The UV-visible spectra were recorded in TNE (10 mM Tris-HCl, 50 mM NaCl and 1 mM EDTA, pH=7.4) buffer at room temperature to investigate the binding affinity between CT-DNA and the N-doped GQDs. The TNE buffer solution was prepared with triple-distilled water. CT-DNA stock solution was prepared by diluting DNA to TNE buffer and kept at 4 °C for no longer than two days. The UV-visible absorbance at 260 and 280 nm of CT-DNA solution in Tris buffer give a ratio of 1.8–1.9 indicating that the DNA was sufficiently free of protein[32]. Before the absorption spectra were recorded, the N-doped GQDs DNA solutions were incubated at room temperature for 5 min.

DNA-Cleavage experiments

The DNA cleavage activity of the N-doped GQDs was studied by agarose gel electrophoresis method. pBR322 DNA (0.1 μg/μL) in Tris-HCl buffer (10 mM, pH:7.4) treated with the compound at 37 °C for 3 h. To determine the mechanism of cleavage activity H_2O_2 was added to one of the group of mixture as an oxidizing agent. After incubation loading buffer was added and samples were electrophoresed for 1 h at 60 V on 1% agarose gel in TAE (400 mM Tris-HCl, 200 mM Acetate-10 mM EDTA, pH:8.2) buffer. Then, bands were visualized by UV light and photographed.

Antioxidant activity

We studied using the absorbance change at 517 nm to calculate the antioxidant activity of the N-doped GQDs to DPPH[33]. A 20 μg/mL methanol solution was prepared for each measurement of DPPH. Then, N-doped GQDs with different concentrations (10, 20, 40, 60 and 80 μg/mL) were added into the DPPH solutions and allowed to incubate in the dark for 30 min.

Cell viability analysis

Thiazolyl blue colorimetric (MTT) test was used to determine the effects of synthesized GQDs on cells. Mouse embryo fibroblast (NIH-3T3), human lung carcinoma (A549) and human breast adenocarcinoma (MDA-MB-231) were chosen as cell lines. The test was carried out in three stages. Firstly, the cells are produced in flasks in DMEM and RPMI. Cells reaching the appropriate growth stage were removed from the flask and approximately 5×10^3 cells was seeded into 96-well plates (Greiner CellStar, Sigma-Aldrich, Germany) and incubated for 24 h at incubator containing 5% CO_2. Following a one-day reproductive period, N-Doped GQDs at certain concentrations were administered with cell culture medium onto the cells and incubated for 24–48 h again. At the end of the incubation periods, MTT strain was added to the well after removing cell culture medium containing the GQDs in the well and allowed to incubate for 4 h. After 4 h, the medium contents were decanted and the formed formazan salt was dissolved in 200 μL of DMSO. The color changes were measured as absorbance at 570 nm with the microplate reader (Cytation 5, BioTek Instruments, Germany). All analyses were repeated in triplicate. The cells which were contain only cell culture medium were used as a control where cell viability was presumed 100%. The absorbance measured in wells containing GQDs were calculated according to the absorbance of the control cells. The IC_{50} values (50% inhibitory concentrations) of N-Doped GQDs on cells were determined. All results were given as mean ± standard error of the mean on the graph[34].

Results and Discussion

UV-visible and FTIR studies

The UV-visible spectrum of the N-doped GQDs was studied in water. The absorption spectra of the N-doped GQDs are shown in Fig. 1. In the spectrum, strong absorption bands at 291 and 319 nm, and a weak absorption band at 375 nm were observed. GQDs, which exhibit photoluminescence, were found

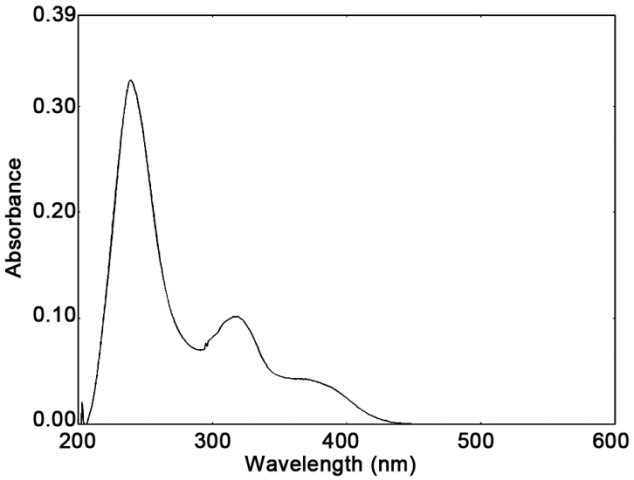

Fig. 1 — UV-visible spectrum of N-doped GQDs.

to show weak absorption above 340 nm[35]. The weak band at 375 nm is due to photoluminescence of N-doped GQDs. As shown in Scheme 1, the aqueous solution of N-doped GQDs is gray in daylight and bright turquoise under 365 nm UV light. This is consistent with the fluorescence of N-doped GQDs. The excitation wavelength dependence of the emission wavelength and intensity is normal in carbon-based fluorescent materials. This behavior results from the distribution of particles in different emitter regions on each nanoparticle. Furthermore, the common peak of the n–π* transition is strong due to the bonds C=N, C=O and P=O. This proves that N-doped GQD occurs at a high rate. Based on the UV-visible spectral results, the change in fluorescent properties of GQDs prepared from citric acid can be easily seen. The absorption spectrum of the N-doped GQDs shows two bands at 289 and 319 nm, which are assigned to the π–π* and n–π* transitions of C=C, C=N, C=O and P=O (Fig. 1).

The FTIR spectra of the N-doped GQDs exhibit characteristic changes in the functional group frequencies when compared with the spectrum of the starting materials, 2-aminoethylphosphinic acid (2-AEPA) and citric acid (CA) (Fig. 2). The NH_2, COOH, C-H, O=P-OH, C=O, C-N, C-O and P-O vibration bands are observed at 3406, 3373, 2904−2873, 2695−2643−2118, 1731, 1638, 1392 and 1085−1032−942 cm^{-1}, respectively in the starting materials. The OH + NH + COOH, C-H, O=P-OH, C=O, C-N, C-O and P-O vibration bands are observed at 3410, 2962, 2444−2395, 1732, 1646, 1401 and 1116−1066−1008 cm^{-1}, respectively in N-doped GQDs (Fig. 2). The frequency of the NH, COOH, C=O, C-N, C-O and P-O bonds shifted to higher values in the N-doped GQDs.

TEM, EDX and DLS studies

The structure and morphology of N-doped GQDs were investigated by TEM. The TEM image is shown in Fig. 3. As can be seen from Fig. 3, the spherical shape of the N-doped GQDs nanoparticle is between 20 and 27 nm in size.

DLS measurements were performed after suspension of N-doped GQDs in DI water. DLS results are given as the mean values of ten consecutive measurements. Each measurement was repeated at least three times. The particle sizes of N-doped GQDs were found to be 27.9±1.5 nm and the results are given in Fig. 4. The particle size measured with DLS is similar or slightly larger than that found with TEM. The DLS experiment shows that the particle size distribution is in the range of 20.9±1.5 nm, which is well supported by the TEM analysis. DLS showed that the particle size was compatible with TEM.

The presence of the elements in the structure of N-doped GQDs was also confirmed by the EDX measurement method. The results of the EDX analysis are given in Fig. 5. Carbon, nitrogen, oxygen and phosphorus were detected on the surface of the

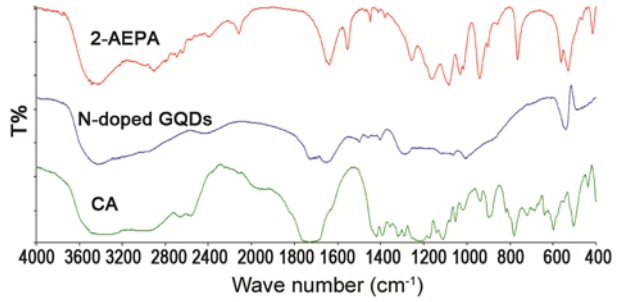

Fig. 2 — FTIR spectra of N-doped GQDs and starting materials.

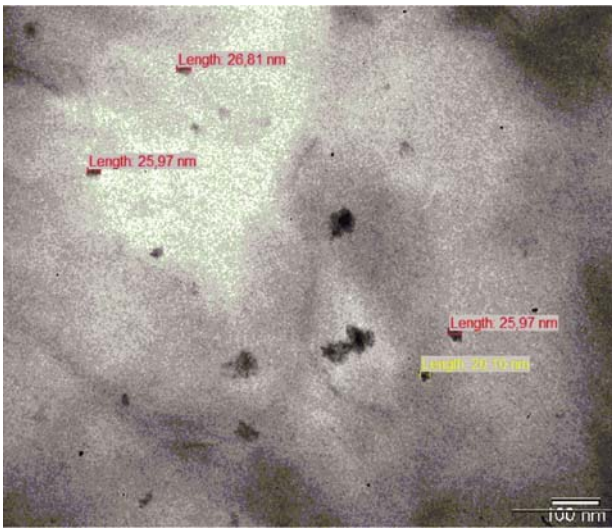

Fig. 3 — TEM image of N-doped GQDs.

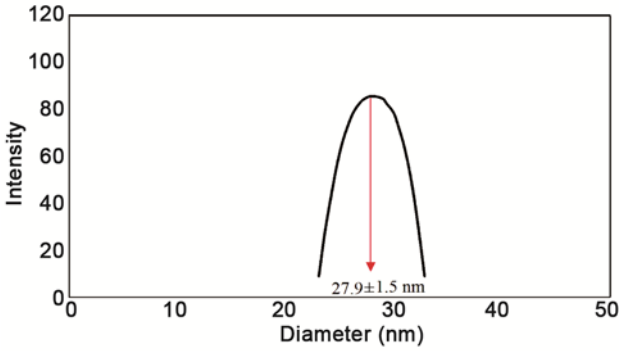

Fig. 4 — DLS analysis of N-doped GQDs.

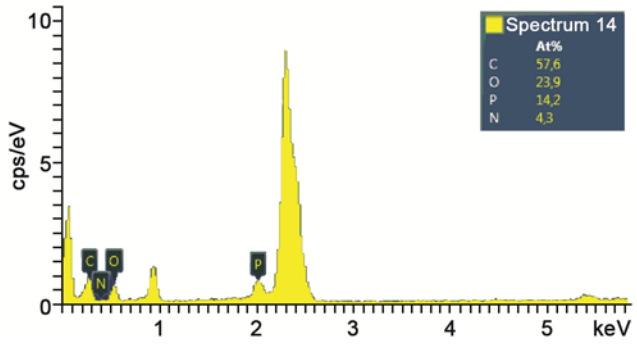

Fig. 5 — EDX analysis of N-doped GQDs.

nanoparticles and the presence of nitrogen and phosphorus on the surface is a striking difference. It is impossible to perform a complete elemental analysis with EDX. Here EDX only gives the content of the elements on the surface. Nevertheless, the EDX data confirm the presence of nitrogen and phosphorus in the compound. The analysis results show that N-doped GQDs were synthesized.

Interaction of N-doped GQDs with DNA

The change in absorption of N-doped GQDs was investigated by the addition of increasing concentrations of CT-DNA to N-doped GQD solution. The absorption spectra of N-doped GQDs interacting with CT-DNA are given in Fig. 6. UV-visible spectroscopy is one of the methods used to investigate the effect of any material on DNA. If a hypochromic effect is observed in the spectrum, there is an intercalation effect against DNA[36,37]. But if the interaction of the material with the DNA is electrostatically or partially intercalative, a hyper-chromic effect is observed in the spectrum. In addition, the red and/or blue shift of the maximum absorption shows that the difference between the HOMO and LUMO energy levels is reduced and the material interacts with the DNA[38,39]. With the increasing concentration of CT-DNA, hypsochromism of 15–98% and lower wavelength of 1–5 nm are observed at 291 nm. Hypsochromicity and blue shift in the spectrum show that CT-DNA interacts with GQDs. According to the absorption results, GQDs interact with CT-DNA via intercalative binding.

DNA-Cleavage studies

The cleavage activity of GQDs was studied by agarose gel-electrophoresis using plasmid pBR322 DNA. In this study, solutions of the compound at concentrations of 1 to 40 µg/mL were used. When DNA was incubated with GQDs, SC (supercoiled)

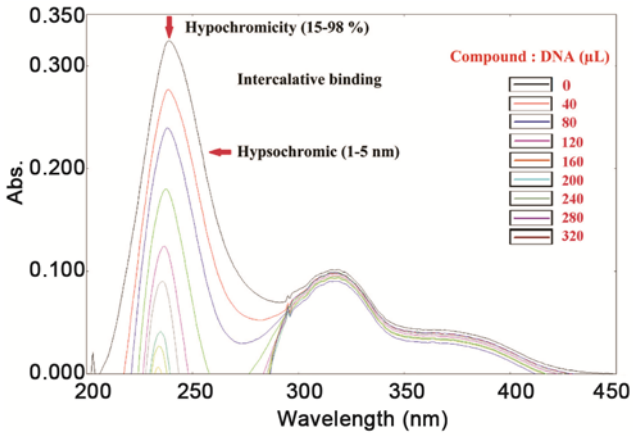

Fig. 6 — UV-visible spectra of the GQDs interaction with CT-DNA.

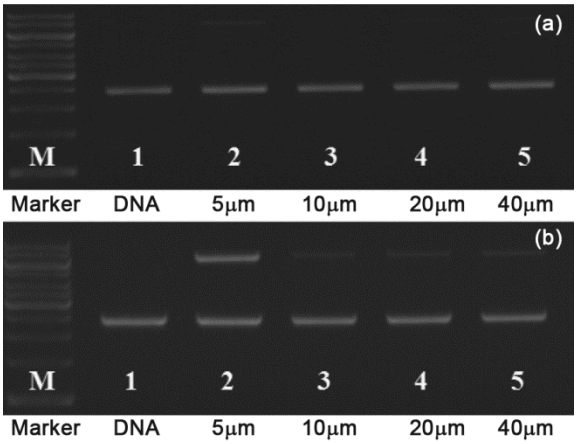

Fig. 7 — Agarose gel electrophoresis patterns for the (a) hydrolytic and (b) oxidative cleavage of pBR322 DNA by GQDS.

DNA was degraded to NC (nicked) form in the presence of H_2O_2. However, hydrolytic cleavage of SC DNA was not observed by N-doped GQDs. The oxidative cleavage activity of N-doped GQDs in the presence of H_2O_2 started at 5 µg/mL concentration of GQDs. The catalytic cleavage activity of the N-doped GQDs is shown in Fig. 7.

Antioxidant activity

Antioxidant activity of N-doped GQDs was studied with the DPPH assay. Upon addition of N-doped GQDs, the solution color changes and the absorbance density of the DPPH methanol solutions at 517 nm is reduced (Fig. 8). The antioxidant activities of 33%, 39.0%, 53.0%, 61.4%, and 75% are obtained (average of three experiments) for N-doped GQDs concentrations of 10, 20, 40, 60, and 80 µg/mL, respectively[40]. The antioxidant activity increases when the concentration of N-doped GQDs increases

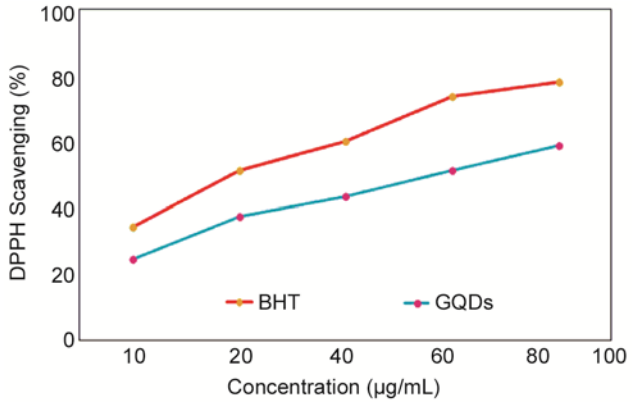

Fig. 8 — Antioxidant activity of N-doped GQDs.

from 10 to 80 µg/mL. The concentration dependent antioxidant activity of N-doped GQDs is consistent with that of graphene quantum dots and carbon nanodots.

Cell viability of N-doped GQDs

Cytotoxicity studies are carried out to determine whether a substance has cytotoxic potential. Cell-based cytotoxicity studies were designed as an alternative to animal experiments because of their ease of administration as well as their compatibility with data from in vivo studies. Characterization of chemicals that promote or inhibit cell proliferation are important areas of cell biology and drug discovery research. During the experiment, changes in the viability of the cells are observed depending on the dose of the substance examined and the duration of exposure. Thiazolyl blue colorimetric (MTT) assay is one of the methods used to detect cell viability[41]. The cell growth inhibition effect and IC_{50} results of N-doped GQDs are presented in Fig. 9 and Table 1.

According to the MTT test results, concentration and time dependent cell viability decrease is observed for the cells. This decrease is especially seen in NIH-3T3 cells, while the least affected cells are A549 cells. Accordingly, 70% cell viability was observed at 228 µg/mL for A549 cells, 200 µg/mL for MDA-MB-231, and 140 µg/mL for NIH-3T3 in the first 24 h. In the 48th h, especially, cell viability values were further decreased for MDA-MB-231 and more affected than NIH-3T3 cells. In the analyses, it was observed that MDA-MB-231 was more affected than A549 cells ($p < 0.05$). In addition to increasing doses, the incubation time also had a statistically significant effect on MDA-MB-231 ($p < 0.05$).

Graphene quantum dots are unique structures for biological imaging due to their unique

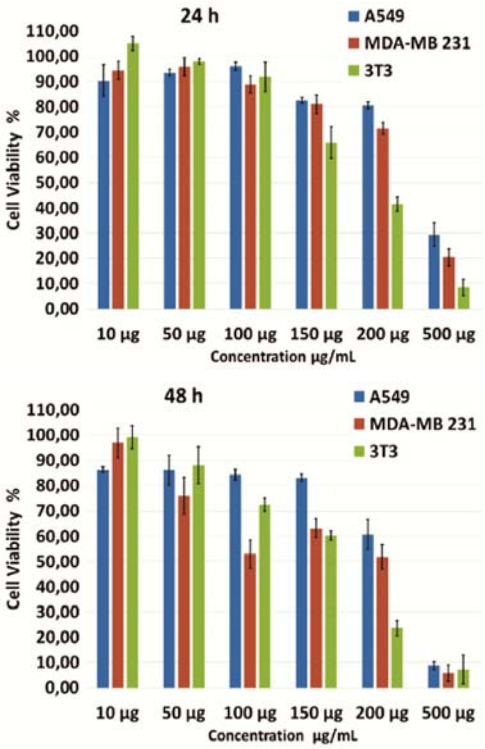

Fig. 9 — Cell viability results of N-doped GQDs after 24 h and 48 h incubation time.

Table 1 — IC_{50} values of N-doped-GQDs on cells

	IC_{50} Values µg/mL	
	24 h	48 h
A549	365 ± 1.20	225 ± 5.50
MDA-MB-231	315 ± 0.75	205 ± 2.10
NIH-3T3	195 ± 2.30	175 ± 0.63

photoluminescent properties. However, functional groups on the surface of GQDs affect the fluorescence spectra and their yield efficiency. Therefore, altering the activity of GQDs with different chemical groups affects the distribution and cytotoxicity, but the lack of studies in this area is an important shortcoming in this area. Random distribution of GQDs within the cell is one of the important factors affecting cytotoxicity. Therefore, the data obtained from these studies are important to decrease the cytotoxicity of GQDs, increase their biocompatibility, and increase their use in biomedical fields[29,42,43].

Conclusions

The synthesis, characterization and applications of N-doped GQDs were reported. The synthesized N-doped GQDs were tested for DNA binding, the DNA cleavage, cell viability and antioxidant activities. The N-doped GQDs showed dose dependent

antioxidant activity and dose-time dependent cell viability. The UV-visible spectra results show that the N-doped GQDs bind to DNA via intercalation mode. The DNA cleavage study showed that the GQDs cleaved DNA oxidatively. The results of this study showed that N-doped GQDs are important molecules with in vitro effects such as growth inhibition of cells, DNA interactions and antioxidant activity. Therefore, they are promising as potential agents for future drug research and development or for use in various biomedical processes.

References

1 Zhao M, *Appl Sci,* 8 (2018) 1303.

2 Chen F, Gao W, Qiu X, Zhang H, Liub L, Liao P, Fu W & Luo Y, *Frontiers in Laboratory Medicine*, 1 (2017) 192.

3 Zou X, Zhang L, Wang Z & Luo Y, *J Am Chem Soc*, 138 (2016) 2064.

4 Li L, Wu G, Yang G, Peng J, Zhao J & Zhu J-J, *Nanoscale*, 5 (2013) 4015.

5 Sun H, Wu L, Wei W & Qu X, *Mater Today*, 16 (2013) 433.

6 Zhou X, Zhang Y, Wang C, Wu X, Yang Y, Zheng B, Wu H, Guo S & Zhang J, *ACS Nano*, 6 (2012) 6592.

7 Tabish T A, Scotton C J, Ferguson D C J, Lin L, van der Veen A, Lowry S, Ali M, Jabeen F, Ali M, Winyard P G & Zhang S, *Nanomedicine,* 13 (2018) 1923.

8 Gong P, Wang J, Hou K, Yang Z, Wang Z, Liu Z, Han X & Yang S, *Carbon*, 112 (2017) 63.

9 Qian Z S, Shan X Y, Chai L J, Chen J R & Feng H, *Biosens Bioelectr*, 68 (2015) 225.

10 Tabish T A, Pranjol M Z I, Karadag I, Horsell D W, Whatmore J L & Zhang S, *Int J Nanomed*, 13 (2018) 1525.

11 Iannazzo D, Pistone A, Salamò M, Galvagno S, Romeo R, Giofré S V, Branca C, Visalli G & Di Pietro A, *Int J Pharm*, 518 (2017) 192.

12 Zhang R & Ding Z, *J Anal Test*, 2 (2018) 45.

13 Kuo W-S, Chen H-H, Chen S-Y, Chang C-Y, Chen P-C, Hou Y-I, Shao Y-T, Kao H-F, Hsu C-L L, Chen Y-C, Chen S-J, Wu S-R & Wang J-Y, *Biomaterials*, 120 (2017) 185.

14 Reina G, G-Domínguez J M, Criado A, Vázquez E, Bianco A & Prato M, *Chem Soc Rev*, 46 (2017) 4400.

15 Tabish T A & Zhang S, Graphene quantum dots: syntheses, properties, and biological applications. In: Hashmi S, ed. *Reference Module in Materials Science and Materials Engineering. Oxford: Elsevier* (2016) 1.

16 Ding H, Zhang F, Zhao C, Lv Y, Ma G, Wei W & Tian Z, *ACS Appl Mater Interfaces*, 9 (2017) 27396.

17 Wang Y, Kong W, Wang L, Zhang J Z, Li Y, Liu X & Li Y, *Phys Chem Chem Phys*, 21 (2019) 1336.

18 Zhao L, Wang Y & Li Y, *Nanomaterials*, 9 (2019) 1708.

19 Zheng X T, Ananthanarayanan A, Luo K Q & Chen P, *Small,* 11 (2015) 1620.

20 Ruiz V, Yate L, García I, Cabanero G & Grande H J, *Carbon*, 116 (2017) 366.

21 Anooj E S & Praseetha P K, *Int J Rec Tech Eng*, 7 (2019) 144.

22 Kholikov K, Ilhom S, Sajjad M, Smith M E, Monroe J D, San O & Er A O, *Photodia and Photody Therapy*, 24 (2018) 7.

23 Szunerits S & Boukherroub R, *J Mater Chem B*, 4 (2016) 6892.

24 Sui X, Luo C, Wang C, Zhang F, Zhang J & Guo S, *Nanomed: Namoted Bio Med*, 12 (2016) 1997.

25 Szunerits S & Boukherroub R, *J Mater Chem B*, 4 (2016) 6892.

26 Wang M, Chen J, Liu C, Qiu J, Wang X, Chen P & Xu C, *Small*, 13 (2017) 1700.

27 Lee W C, Haley C, Lim Y X, Shi H, Lena A, Tang L, Wang Y, Lim C T & Loh K P, *ACS Nano*, 5 (2011) 7334.

28 Yuan X, Liu Z, Guo Z, Ji Y, Jin M & Wang X, *Nanoscale Res Lett,* 9 (2014) 1.

29 Jiang D, Chen Y, Li N, Li W, Wang Z, Zhu J, Zhang H, Liu B & Xu S, *Plos one*, 12: e0144906 (2015) 1.

30 Ogi T, Iwasaki H, Aishima K, Iskandar F, Wang W N, Takimiya K & Okuyama K, *RSC Adv*, 4 (2014) 55709.

31 Naik J P, Sutradhar P & Saha M, *J Nanostruct Chem*, 7 (2017) 85.

32 Marmur J, *J Mol Biol*, 3 (1961) 208.

33 Garcia E J, Oldoni T L C, Alencar S M D, Reis A, Loguercio A D & Grande R H M, *Braz Dent J*, 23 (2012) 22.

34 Senel B, Büyükköroğlu G & Yazan Y, *Pharmazie*, 70 (2015) 698.

35 Qu D, Zheng M, Zhang L, Zhao H, Xie Z, Jing X, Haddad R E, Fan H & Sun Z, *Scientific Reports*, 4 (2014) 5294

36 Barare B, Yıldız M, Alpaslan G, Dilek N, Ünver H, Tadesse S & Aslan K, *Sens Actu B: Chem*, 215 (2015) 52.

37 Barare B, Yıldız M, Ünver H & Aslan K, *Tetrahedron Lett,* 57 (2016) 537.

38 Yıldız M, Karpuz O, Zeyrek C T, Boyacıoğlu B, Dal H, Demir N, Yıldırım N & Unver H, *J Mol Struct*, 1094 (2015) 148.

39 Ünver H, Boyacıoglu B, Zeyrek C T, Yıldız M, Demir N, Yıldırım N, Karaosmanoglu O, Sivas H & Elmalı A, *J Mol Struct*, 1125 (2016) 162.

40 Huang D J, Ou B X & Prior R L, *J Agr Food Chem*, 53 (2005) 1841.

41 Eastman A, *Oncotarget,* 8 (2017) 8854.

42 Yuan X, Liu Z, Guo Z, Ji Y, Jin M & Wang X, *Nanoscale Res Lett,* 9 (2014) 1.

43 Şenel B, Demir N, Büyükköroğlu G & Yıldız M, *Saudi Pharm J*, 27 (2019) 846.